



HAL
open science

Coherence in the radial degree of freedom

Abhinandan Bhattacharjee, Shrestha Biswas, Miguel A Alonso, Anand K Jha

► **To cite this version:**

Abhinandan Bhattacharjee, Shrestha Biswas, Miguel A Alonso, Anand K Jha. Coherence in the radial degree of freedom. *Journal of the Optical Society of America. A Optics, Image Science, and Vision*, 2023, 40 (3), pp.411-416. 10.1364/josaa.474724 . hal-04020857

HAL Id: hal-04020857

<https://hal.science/hal-04020857>

Submitted on 9 Mar 2023

HAL is a multi-disciplinary open access archive for the deposit and dissemination of scientific research documents, whether they are published or not. The documents may come from teaching and research institutions in France or abroad, or from public or private research centers.

L'archive ouverte pluridisciplinaire **HAL**, est destinée au dépôt et à la diffusion de documents scientifiques de niveau recherche, publiés ou non, émanant des établissements d'enseignement et de recherche français ou étrangers, des laboratoires publics ou privés.



Coherence in the radial degree of freedom

ABHINANDAN BHATTACHARJEE,^{1,*} SHRESTHA BISWAS,¹ MIGUEL A. ALONSO,^{1,2,3} AND ANAND K. JHA^{1,4}

¹Department of Physics, Indian Institute of Technology Kanpur, Kanpur, UP 208016, India

²Aix Marseille Université, CNRS, Centrale Marseille, Institut Fresnel, UMR 7249, 13397 Marseille Cedex 20, France

³The Institute of Optics and the Center for Coherence and Quantum Optics, University of Rochester, Rochester, New York 14627, USA

⁴e-mail: akjha@iitk.ac.in

*Corresponding author: arko.hkd@gmail.com

Received 2 September 2022; revised 4 December 2022; accepted 14 December 2022; posted 22 December 2022; published 6 February 2023

Coherence quantifies the statistical fluctuations in an optical field and has been extensively studied in the space, time, and polarization degrees of freedom. In the context of space, coherence theory has been formulated between two transverse positions as well as between two azimuthal positions, referred to as transverse spatial coherence and angular coherence, respectively. In this paper, we formulate the theory of coherence for optical fields in the radial degree of freedom and discuss the associated concepts of coherence radial width, radial quasi-homogeneity, and radial stationarity with some physically realizable examples of radially partially coherent fields. Furthermore, we propose an interferometric scheme for measuring radial coherence. © 2023 Optica Publishing Group

<https://doi.org/10.1364/JOSAA.474724>

1. INTRODUCTION

Optical coherence theory is a well-established research domain aimed at understanding and characterizing the statistical fluctuations in an optical field [1,2]. Optical fields having partial coherence have found applications in several areas including imaging through scattering media [3–5], optical coherence tomography [6–8], and optical communication [8,9]. Coherence in a given degree of freedom, such as time, space, or polarization, is defined through two-point cross-spectral density [1,10]. In the context of space, coherence theory has been formulated between two transverse positions [1,10], and it is referred to as transverse spatial coherence. Several experimental schemes have been developed for measuring the transverse spatial coherence of optical fields [10–15].

The electric field at a transverse point in Cartesian coordinates (x, y) can be written in the cylindrical coordinate system as $E(r, \theta)$, where $x = r \cos \theta$ and $y = r \sin \theta$. Thus the cross-spectral density of a monochromatic field in the cylindrical coordinate system can be written as $W(r_1, \theta_1, r_2, \theta_2) = \langle E^*(r_1, \theta_1) E(r_2, \theta_2) \rangle_e$, where $\langle \dots \rangle_e$ represents the ensemble average, and $E(r_1, \theta_1)$ and $E(r_2, \theta_2)$ represent the electric fields at locations (r_1, θ_1) and (r_2, θ_2) , respectively, where the polar coordinates are defined with respect to the center of the coordinate system. Recent work has focused on different classes of fields based on their description in cylindrical coordinates. This has included studies of fields whose degree of coherence depends only on the azimuthal separation [16], radial separation [17], or difference in the squares of radial coordinates [18]. A representation of generic cross-spectral

densities in terms of the radial variable and orbital angular momentum (OAM) was also proposed recently [19].

A measure of coherence that focuses on the angular degree of freedom was proposed based on averaging over the radial coordinate [20,21]. Efficient experimental measurement of this angular coherence function has led to several important applications, including measurement of the OAM spectrum of light [21], measurement of the angular Schmidt spectrum of OAM-entangled photons [22], and state tomography of high-dimensional OAM states of photons [23]. Lately, there have been increased efforts for utilizing the radial degree of freedom for applications in optical communication and quantum information [24–27]. We explore in this paper the counterpart in the radial degree of freedom of the angular measure in [20,21], where now the averaging takes place over the azimuthal variable. The paper is organized as follows. In Section 2, we define the radial cross-spectral density and associated concepts of coherence radial width, radial quasi-homogeneity, and radial stationarity. In Section 3, we discuss these concepts with a few physically realizable examples of radially partially coherent fields. In Section 4, we propose an interferometric method for measuring the degree of radial coherence. Section 5 contains the conclusion.

2. RADIAL CROSS-SPECTRAL DENSITY

When the cross-spectral density is averaged over the radial degree of freedom, one obtains the angle cross-spectral density as $W(\theta_1, \theta_2) = \int r dr W(r, \theta_1, r, \theta_2)$ [20,21]. As mentioned earlier, efficient experimental measurements of this function

have been implemented [21–23]. In an analogous manner, for defining the cross-spectral density in the radial degree of freedom, we take $\theta_1 = \theta_2 = \theta$ and average $W(r_1, \theta_1, r_2, \theta_2)$ over the azimuthal degree of freedom to obtain

$$W_R(r_1, r_2) \equiv \frac{1}{2\pi} \int_{-\pi}^{\pi} W(r_1, \theta, r_2, \theta) d\theta. \quad (1)$$

The function $W_R(r_1, r_2)$ is then called the radial cross-spectral density (in analogy to the azimuthal cross-spectral density), and it quantifies the correlation between fields at two separate radial positions, r_1 and r_2 . In situations in which the complete cross-spectral density is separable in its radial and azimuthal coordinates, so that $W(r_1, \theta, r_2, \theta) = W_R(r_1, r_2) f(\theta)$, we can write the radial cross-spectral density $W_R(r_1, r_2)$ as

$$W_R(r_1, r_2) = \sqrt{I_R(r_1)I_R(r_2)} \mu_R(r_2, r_1), \quad (2)$$

where

$$\mu_R(r_1, r_2) = \frac{W_R(r_1, r_2)}{\sqrt{I_R(r_1)I_R(r_2)}} \quad (3)$$

is the complex degree of radial coherence, and its magnitude $|\mu_R(r_1, r_2)|$ can be referred to as the degree of radial coherence. $I_R(r) = W_R(r, r) = \frac{1}{2\pi} \int_{-\pi}^{\pi} W(r, \theta, r, \theta) d\theta$ is the radial intensity distribution. Figure 1 illustrates the concept of radial cross-spectral density. The degree of coherence $|\mu_R(r_1, r_2)|$ quantifies the correlation between fields at radial coordinates r_1 and r_2 , and it lies between zero and one. If $\mu_R(r_1, r_2)$ depends only on the difference $\Delta r = r_2 - r_1$ and the radial intensity distribution $I_R(r)$ varies slowly compared to the variations in $\mu_R(\Delta r)$ as a function of Δr , then the field can be said to be radially quasi-homogeneous. For a radially quasi-homogeneous field, if $I_R(r)$ is constant, the field can be referred to as radially homogeneous, or using the terminology in [21,28–31], it can also be referred to as radially stationary. Thus, for a radially stationary field, we get

$$I_R(r) = I_0 \quad \text{and} \quad W_R(r_1, r_2) = I_0 \mu_R(r_2 - r_1) = I_0 \mu_R(\Delta r), \quad (4)$$

where I_0 is a constant. The width of $|\mu_R(\Delta r)|$ as a function of Δr can be referred to as the coherence radial width σ_{rad} , which can be seen as a measure of the radial length scale over which the field has appreciable correlations. For a radially perfectly coherent field, σ_{rad} is ∞ , and for a radially incoherent field, σ_{rad} is zero.

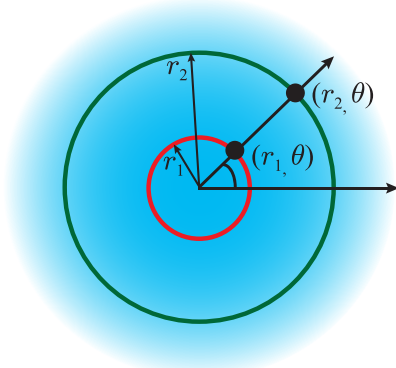


Fig. 1. Illustrating radial coherence. The cross-spectral density $W(r_1, \theta, r_2, \theta)$ is averaged over the azimuthal coordinate θ to obtain the radial cross-spectral density $W_R(r_1, r_2)$.

Please note that the interpretation of $|\mu_R(r_1, r_2)|$ as a radial degree of coherence is valid only for certain classes of fields; counterexamples include fully coherent fields without rotational symmetry about the chosen origin, for which $|\mu_R(r_1, r_2)|$ can be considerably less than unity. For cases in which the cross-spectral density is separable in polar coordinates, the radial part is precisely the radial cross-spectral density. One example is that of fields with definite OAM for which the nonzero elements of the coherence–OAM matrix defined in [19] reduce to the radial cross-spectral density.

3. EXAMPLES OF RADIALLY PARTIALLY COHERENT FIELDS

We now consider the measures of radial coherence mentioned earlier for a few representative examples of physically realizable radially partially coherent fields.

A. Field in the Form of an Incoherent Mixture of Laguerre–Gaussian Modes

We consider an incoherent mixture of Laguerre–Gaussian (LG) $\text{LG}_p^{l=0}(r)$ [32] modes as an example of a radially partially coherent field that is fully independent of the azimuthal angle. The mixture consists only of $l = 0$ mode, and the proportion of a mode with index p is λ_p . The radial cross-spectral density in this case can be written as

$$W_R(r, r + \Delta r) = \sum_{p=0}^{p_{\text{max}}} \lambda_p \text{LG}_p^{*l=0}(r) \text{LG}_p^{l=0}(r + \Delta r), \quad (5)$$

where $\text{LG}_p^{l=0}(r) = A \left[\frac{\sqrt{2r}}{w} \right] L_p^{l=0}(2r^2/w^2) \exp[-r^2/w^2]$, and w is the beam waist [32]. Since this cross-spectral density has no explicit dependence on azimuthal coordinates, it remains unchanged after averaging over the azimuthal degree of freedom, as defined in Eq. (1). The corresponding radial intensity distribution $I_R(r)$ and degree of coherence function $|\mu_R(r, r + \Delta r)|$ can be written as

$$I_R(r) = \sum_{p=0}^{p_{\text{max}}} \lambda_p |\text{LG}_p^{l=0}(r)|^2 \quad (6)$$

and

$$|\mu_R(r, r + \Delta r)| = \frac{\left| \sum_{p=0}^{p_{\text{max}}} \lambda_p \text{LG}_p^{l=0}(r) \text{LG}_p^{*l=0}(r + \Delta r) \right|}{\sqrt{\left[\sum_{p=0}^{p_{\text{max}}} \lambda_p |\text{LG}_p^{l=0}(r)|^2 \right] \left[\sum_{p=0}^{p_{\text{max}}} \lambda_p |\text{LG}_p^{l=0}(r + \Delta r)|^2 \right]}}. \quad (7)$$

Figure 2(a) shows plots of numerically evaluated $I_R(r)$ as a function of r , and of $|\mu_R(r, r + \Delta r)|$ as a function of Δr . For the plots, we take $\lambda_p = 1/p_{\text{max}}$, $p_{\text{max}} = 20$, and $w = 0.4$ mm. We note that $|\mu_R(r, r + \Delta r)|$ depends on both r and Δr . This implies that the field is neither stationary nor quasi-homogeneous and thus that the coherence radial width σ_{rad} does depend on r . We also note that LG modes $\text{LG}_p^{l=0}(r)$ are self-similar under paraxial propagation, and therefore, the shape

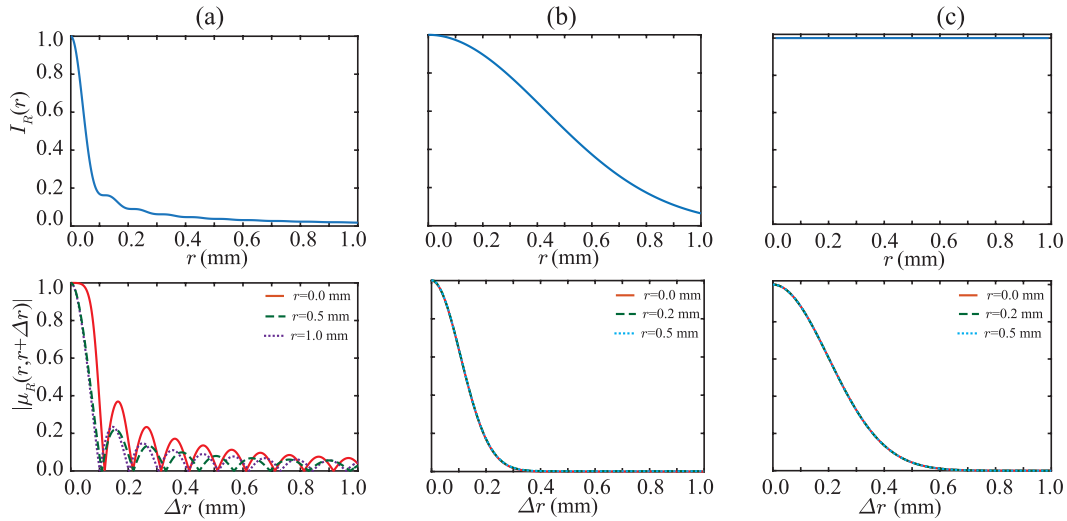


Fig. 2. Radial intensity distribution $I_R(r)$ as a function of r and the degree of coherence $|\mu_R(r, r + \Delta r)|$ as a function of Δr for various radially partially coherent fields: (a) incoherent mixture of LG modes, (b) GSM field, and (c) incoherent mixture of transverse plane-wave modes.

of an LG mode does not change upon propagation except for an overall increase in beam size and the corresponding attenuation in intensity. Therefore, the functional forms of the above radial intensity and the degree of coherence functions do not change upon propagation, but the beam size and the coherence radial width do increase upon propagation. One can experimentally generate such radially partially coherent fields by using the method described in [33].

B. Radial Gaussian Schell Model Fields

Gaussian Schell model (GSM) fields are widely used models of quasi-homogeneous partially coherent fields [34–36]. Therefore, as a second example, we consider a GSM field in the radial degree of freedom and write the cross-spectral density as

$$W_R(r_1, r_2) = \exp\left[-\frac{r_1^2 + r_2^2}{4\sigma_s^2}\right] \exp\left[-\frac{(r_2 - r_1)^2}{2\sigma_{\text{rad}}^2}\right]. \quad (8)$$

As for the previous example, the cross-spectral density is independent of azimuthal coordinates, and therefore, it remains unchanged after averaging over the azimuthal degree of freedom in Eq. (1). The corresponding radial intensity distribution $I_R(r)$ and the degree of coherence $|\mu_R(r, r + \Delta r)|$ are given by

$$I_R(r) = \exp\left[-\frac{r^2}{2\sigma_s^2}\right] \quad \text{and} \quad |\mu_R(r, r + \Delta r)| = \exp\left[-\frac{(\Delta r)^2}{2\sigma_{\text{rad}}^2}\right], \quad (9)$$

where σ_s and σ_{rad} are the radial beam size and coherence radial width, respectively. We note that the degree of coherence $|\mu_R(r, r + \Delta r)|$ depends only on separation Δr . Therefore, in situations in which $\sigma_s \gg \sigma_{\text{rad}}$, the above cross-spectral density is radially quasi-homogeneous. However, except in the limit $\sigma_s \rightarrow \infty$, the field is not radially stationary. Following the method worked out in [35], we write the radial GSM field as an incoherent mixture of radial Hermite Gaussian (HG) functions $HG_p(r)$ [17], with λ_p being the proportion:

$$W_R(r, r + \Delta r) = \sum_{p=0}^{p_{\text{max}}} \lambda_p HG_p^*(r) HG_p(r + \Delta r). \quad (10)$$

Here $HG_p(r) = AH_p\left[\frac{\sqrt{2}r}{w}\right] \exp[-r^2/w^2]$, A is a constant, w is the beam waist, $\lambda_p = \frac{1}{[(Q/2)^2 + 1 + Q\sqrt{(Q/2)^2 + 1}]^p}$, and $Q = \sigma_{\text{rad}}/2.25\sigma_s$. Figure 2(b) shows plots of numerically evaluated $I_R(r)$ as a function of r , and of $|\mu_R(r, r + \Delta r)|$ as a function of Δr . For these plots, we used $p_{\text{max}} = 50$, $Q = 0.5$, and $w = 0.3$ mm. We note from the plots that the field is indeed radially quasi-homogeneous. Note, however, that the radial HG functions are not self-similar solutions of the paraxial wave equation. As a result, the functional forms of the above radial intensity distribution and the degree of coherence change considerably upon propagation. Moreover, from the recent theoretical study in [17] of an analogous radially partially coherent field, we expect that both beam size and coherence radius increase upon propagation. The above radial GSM field can also be physically realized by using the method described in [33].

C. Field in the Form of an Incoherent Mixture of Transverse Plane-Wave Modes

It turns out that fields for which the cross-spectral density is separable in polar coordinates are not the only ones for which the definition of radial coherence is meaningful, as we show now with a simple example. Consider a partially coherent field in the form of an incoherent mixture of plane-wave modes and write the cross-spectral density $\mathcal{W}(x_1, y_1, x_2, y_2)$ as

$$\mathcal{W}(x_1, y_1, x_2, y_2) = \int \lambda(q_x, q_y) e^{i[q_x(x_2 - x_1) + q_y(y_2 - y_1)]} dq_x dq_y, \quad (11)$$

where $\lambda(q_x, q_y)$ is the mode density. Using the transformations $(x_1, y_1) = (r_1 \cos \theta_1, r_1 \sin \theta_1)$, $(x_2, y_2) = (r_2 \cos \theta_2, r_2 \sin \theta_2)$, and $(q_x, q_y) = (q_r \cos q_\theta, q_r \sin q_\theta)$, where q_r and q_θ are radial and azimuthal components of the transverse plane-wave modes (q_x, q_y) , respectively, we write $\mathcal{W}(x_1, y_1, x_2, y_2)$ in the polar coordinates as

$$W(r_1, \theta_1, r_2, \theta_2) = \int q_r \lambda(q_r \cos q_\theta, q_r \sin q_\theta) e^{iq_r \cos q_\theta (r_2 \cos \theta_2 - r_1 \cos \theta_1)} \\ \times e^{iq_r \sin q_\theta (r_2 \sin \theta_2 - r_1 \sin \theta_1)} dq_r dq_\theta. \quad (12)$$

If the mode density is rotationally symmetric, that is, if $\lambda(q_x, q_y) \equiv \lambda(q_r)$, this expression simplifies to

$$W(r_1, \theta_1, r_2, \theta_2) = 2\pi \int q_r \lambda(q_r) \\ \times J_0 \left[q_r \sqrt{r_1^2 + r_2^2 - 2r_1 r_2 \cos(\theta_2 - \theta_1)} \right] dq_r. \quad (13)$$

While this cross-spectral density is not separable in its radial and azimuthal coordinates, it depends on θ_1 and θ_2 only through their difference. Therefore, setting $\theta_1 = \theta_2 = \theta$ gives a result that is unaffected by subsequent angular averaging:

$$W_R(r_1, r_2) = \frac{1}{2\pi} \int W(r_1, \theta, r_2, \theta) d\theta = W_R(r_2 - r_1) = W_R(\Delta r). \quad (14)$$

The intensity and degree of coherence can therefore, be written as

$$I_R(r) = W_R(r, r) = I_0 \quad \text{and} \quad |\mu_R(r, r + \Delta r)| = \frac{|W_R(\Delta r)|}{I_0}, \quad (15)$$

where $W_R(\Delta r)$ and $\lambda(q_r)$ are related by the following Hankel transformation:

$$W_R(\Delta r) = 2\pi \int q_r \lambda(q_r) J_0(q_r \Delta r) dq_r. \quad (16)$$

That is, for this type of field, the coherence between any two points depends only on their separation, and therefore, the coherence for any two points with the same azimuthal variable but different radii depends only on the difference of the radial coordinates. Figure 2(c) shows the plots of numerically evaluated $I_R(r)$ as a function of r and $|\mu_R(r, r + \Delta r)|$ as a function of Δr . For the plots, we have taken $\lambda(q_x, q_y) = \exp \left[-\frac{q_x^2 + q_y^2}{2\sigma_q^2} \right]$, where $\sigma_q = 5 \text{ mm}^{-1}$. We note that the cross-spectral density of Eq. (11) does not depend on the propagation distance z [31].

Therefore, the above radial intensity distribution $I_R(r)$ and the degree of coherence function $|\mu_R(r, r + \Delta r)|$ also remain propagation invariant. The experimental generation of such fields has already been demonstrated in [31].

Note that a similar mathematical result is found even if $\lambda(q_x, q_y)$ is not rotationally symmetric, since setting $\theta_1 = \theta_2 = \theta$ gives

$$W(r_1, \theta, r_2, \theta) = \int q_r \lambda(q_r \cos q_\theta, q_r \sin q_\theta) e^{iq_r \cos q_\theta (r_2 - r_1) \cos \theta} \\ \times e^{iq_r \sin q_\theta (r_2 - r_1) \sin \theta} dq_r dq_\theta, \quad (17)$$

which after angular averaging yields

$$W_R(\Delta r) = \int q_r \lambda(q_r \cos q_\theta, q_r \sin q_\theta) J_0(q_r \Delta r) dq_r dq_\theta. \quad (18)$$

While this radial coherence does depend only on radial separation, this is to be understood only in the sense of an average, and not of the coherence between each pair of points with given radial separation and equal angle.

4. PROPOSED SCHEME FOR MEASURING RADIAL CROSS-SPECTRAL DENSITY

Figure 3(a) shows the schematic of a proposed interferometric scheme for measuring the radial cross-spectral density $W_R(r_1, r_2)$. This scheme is the radial analog of the wavefront-inversion-based scheme for measuring the angular [21] and transverse spatial coherence functions [15]. In our scheme, the field in one arm is magnified $m > 1$ times before interfering, and therefore, the electric field $E_{\text{out}}(r, \theta)$ at the output port of the interferometer can be written as

$$E_{\text{out}}(r, \theta) = \sqrt{k_1} E\left(\frac{r}{m}, \theta\right) e^{i\delta_1} + \sqrt{k_2} E(r, \theta) e^{i\delta_2}, \quad (19)$$

where δ_1 and δ_2 are the phases acquired by the field in the two interferometer arms, and k_1 and k_2 are the scaling factors. The intensity at the output port of the interferometer $I_{\text{out}}^\delta(r, \theta) = \langle E_{\text{out}}^*(r, \theta) E_{\text{out}}(r, \theta) \rangle$ can be written as

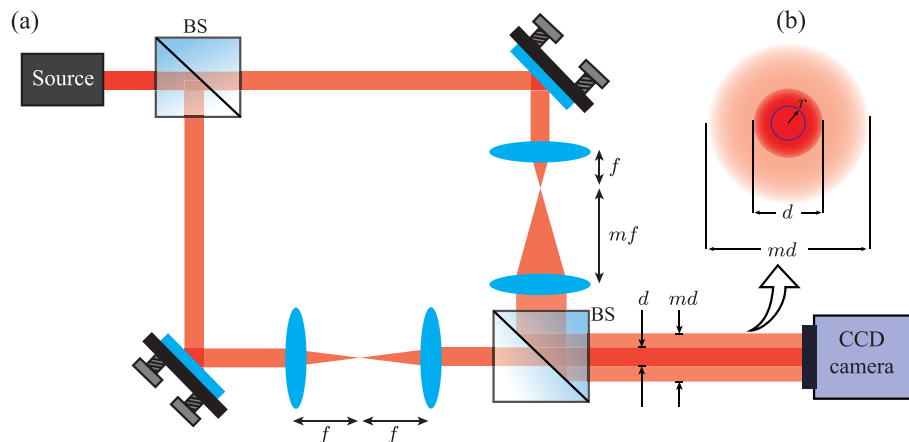


Fig. 3. (a) Schematic of the interferometer for measuring the radial cross-spectral density $W_R(r, r/m)$ of a source field. (b) Transverse cross section of the interfering fields at the camera plane.

$$I_{\text{out}}^{\delta}(r, \theta) = k_1 I(r/m, \theta) + k_2 I(r, \theta) + 2\sqrt{k_1 k_2} \\ \times (\text{Re}[W(r, \theta, r/m, \theta)] \cos \delta \\ - \text{Im}[W(r, \theta, r/m, \theta)] \sin \delta), \quad (20)$$

where $\delta = (\delta_2 - \delta_1)$, and $\text{Re}[\cdot \cdot \cdot]$ and $\text{Im}[\cdot \cdot \cdot]$ are the real and imaginary parts, respectively. By recording the interferogram at four different values of δ , namely, $\delta = 0$, $\delta = \pi/2$, $\delta = \pi$, and $\delta = 3\pi/2$, one can measure the real and imaginary parts as

$$\text{Re}[W(r, \theta, r/m, \theta)] \propto [I^{\delta=0}(r, \theta) - I^{\delta=\pi}(r, \theta)], \quad (21)$$

$$\text{Im}[W(r, \theta, r/m, \theta)] \propto [I^{\delta=\pi/2}(r, \theta) - I^{\delta=3\pi/2}(r, \theta)]. \quad (22)$$

Finally, the radial cross-spectral density $W_R(r, r/m)$ can be obtained by averaging $W(r, \theta, r/m, \theta)$ over the azimuthal coordinate θ . The degree of coherence function $|\mu_R(r, r/m)|$ can be obtained by measuring the radial intensities $I_R(r)$ and $I_R(r/m)$ of the two arms and then using the relation $|\mu_R(r, r/m)| = |W_R(r, r/m)|/\sqrt{I_R(r)I_R(r/m)}$. We note that, in general, for measuring $W_R(r, r/m)$, one needs to make the interferometric measurements at a range of values of m . However, if the field is radially quasi-homogeneous or radially stationary, one needs to make measurements at only one value of m .

We note that the performance of the proposed interferometric scheme crucially depends on how accurately the interfering beams coaxially overlap with each other and also on the relative stability of the two interfering beams. These two factors are usually a bit challenging to control in a Mach–Zehnder type interferometer, which has two separate interferometric paths. However, there have been several experimental demonstrations in which good control over these two factors has been demonstrated using Mach–Zehnder type interferometers [15,21,22]. Therefore, our proposed setup seems practically viable. Nonetheless, if a common-path interferometer is used instead of a Mach–Zehnder interferometer, one can get better control of these two factors.

Just as the OAM mode spectrum can be measured by measuring the angular cross-spectral density [20,21], the measurement of radial cross-spectral density can yield the radial mode spectrum in a situation in which the field is an incoherent mixture of perfectly coherent radial modes. We can see it as follows. If the radially partially coherent field is an incoherent mixture of modes $\phi_n(r)$ with radial mode spectrum λ_n , the corresponding radial cross-spectral density $W_R(r_1, r_2)$ is given by

$$W_R(r_1, r_2) = \sum_n \lambda_n \phi_n^*(r_1) \phi_n(r_2). \quad (23)$$

Using the orthogonality relation $\int \phi_n^*(r) \phi_m(r) r dr = \delta_{n,m}$ of $\phi_n(r)$ modes, we obtain λ_n :

$$\lambda_n = \int_{r_1=0}^{\infty} \int_{r_2=0}^{\infty} W_R(r_1, r_2) \phi_n^*(r_1) r_1 dr_1 \phi_n(r_2) r_2 dr_2. \quad (24)$$

Thus, by measuring the radial cross-spectral density $W_R(r_1, r_2)$, one can efficiently measure the radial mode spectrum λ_n .

5. CONCLUSION

In conclusion, in this paper, we have studied a measure of radial coherence that is analogous to angular cross-spectral density [20,21]. For fields in which two-point cross-spectral density is separable in polar coordinates around a specific origin, the radial cross-spectral density defined here corresponds directly to a measure of coherence between a pair of points with equal angular coordinates. However, it was shown that polar separability is not a prerequisite for this angularly averaged measure to represent the true coherence of any pair of points with the same angular coordinate, independently of this coordinate. In addition, we have also proposed an interferometric scheme for measuring the radial cross-spectral density function. Just as spatially partially coherent fields are used for enhancing imaging resolution in the presence of turbulence [3–5], we expect fields with partial radial coherence to have important implications for enhancing the imaging resolution of radial features in an object, especially in the presence of turbulence.

Funding. Department of Science and Technology, Ministry of Science and Technology, India (DST/ICPS/QuST/Theme-1/2019); Science and Engineering Research Board (STR/2021/000035, VJR/2021/000012).

Acknowledgment. We thank Shaurya Aarav for useful discussions. M.A.A. acknowledges the hospitality of IIT Kanpur's Physics Department and financial support during his visit under the VAJRA Faculty Scheme of India's Science and Engineering Research Board.

Disclosures. The authors declare no conflicts of interest.

Data availability. Data underlying the results presented in this paper are not publicly available at this time but may be obtained from the authors upon reasonable request.

REFERENCES

1. L. Mandel and E. Wolf, *Optical Coherence and Quantum Optics* (Cambridge University, 1995).
2. J. W. Goodman, *Statistical Optics* (Wiley, 2015).
3. B. Redding, M. A. Choma, and H. Cao, "Speckle-free laser imaging using random laser illumination," *Nat. Photonics* **6**, 355–359 (2012).
4. B. Redding, A. Cerjan, X. Huang, M. L. Lee, A. D. Stone, M. A. Choma, and H. Cao, "Low spatial coherence electrically pumped semiconductor laser for speckle-free full-field imaging," *Proc. Natl. Acad. Sci. USA* **112**, 1304–1309 (2015).
5. A. Bhattacharjee, S. Aarav, H. Wanare, and A. K. Jha, "Controlling propagation of spatial coherence for enhanced imaging through scattering media," *Phys. Rev. A* **101**, 043839 (2020).
6. B. Karamata, P. Lambelet, M. Laubscher, R. Salathé, and T. Lasser, "Spatially incoherent illumination as a mechanism for cross-talk suppression in wide-field optical coherence tomography," *Opt. Lett.* **29**, 736–738 (2004).
7. J. Kim, D. T. Miller, E. K. Kim, S. Oh, J. H. Oh, and T. E. Milner, "Optical coherence tomography speckle reduction by a partially spatially coherent source," *J. Biomed. Opt.* **10**, 064034 (2005).
8. A. Bhattacharjee and A. K. Jha, "Experimental demonstration of structural robustness of spatially partially coherent fields in turbulence," *Opt. Lett.* **45**, 4068–4071 (2020).
9. D. Peng, Z. Huang, Y. Liu, Y. Chen, F. Wang, S. A. Ponomarenko, and Y. Cai, "Optical coherence encryption with structured random light," *Photonix* **2**, 1 (2021).
10. F. Zernike, "The concept of degree of coherence and its application to optical problems," *Physica* **5**, 785–795 (1938).
11. J. Turunen, A. Vasara, and A. T. Friberg, "Propagation invariance and self-imaging in variable-coherence optics," *J. Opt. Soc. Am. A* **8**, 282–289 (1991).

12. C. Iaconis and I. A. Walmsley, "Direct measurement of the two-point field correlation function," *Opt. Lett.* **21**, 1783–1785 (1996).
13. J. K. Wood, K. A. Sharma, S. Cho, T. G. Brown, and M. A. Alonso, "Using shadows to measure spatial coherence," *Opt. Lett.* **39**, 4927–4930 (2014).
14. M. Santarsiero and R. Borghi, "Measuring spatial coherence by using a reversed-wavefront young interferometer," *Opt. Lett.* **31**, 861–863 (2006).
15. A. Bhattacharjee, S. Aarav, and A. K. Jha, "Two-shot measurement of spatial coherence," *Appl. Phys. Lett.* **113**, 051102 (2018).
16. G. Piquero, M. Santarsiero, R. Martinez-Herrero, J. De Sande, M. Alonzo, and F. Gori, "Partially coherent sources with radial coherence," *Opt. Lett.* **43**, 2376–2379 (2018).
17. J. De Sande, R. Martinez-Herrero, G. Piquero, M. Santarsiero, and F. Gori, "Pseudo-Schell model sources," *Opt. Express* **27**, 3963–3977 (2019).
18. M. Santarsiero, R. Martinez-Herrero, D. Maluenda, J. De Sande, G. Piquero, and F. Gori, "Partially coherent sources with circular coherence," *Opt. Lett.* **42**, 1512–1515 (2017).
19. O. Korotkova and G. Gbur, "Unified matrix representation for spin and orbital angular momentum in partially coherent beams," *Phys. Rev. A* **103**, 023529 (2021).
20. A. K. Jha, G. S. Agarwal, and R. W. Boyd, "Partial angular coherence and the angular Schmidt spectrum of entangled two-photon fields," *Phys. Rev. A* **84**, 063847 (2011).
21. G. Kulkarni, R. Sahu, O. S. Magaña-Loaiza, R. W. Boyd, and A. K. Jha, "Single-shot measurement of the orbital-angular-momentum spectrum of light," *Nat. Commun.* **8**, 1054 (2017).
22. G. Kulkarni, L. Taneja, S. Aarav, and A. K. Jha, "Angular Schmidt spectrum of entangled photons: derivation of an exact formula and experimental characterization for noncollinear phase matching," *Phys. Rev. A* **97**, 063846 (2018).
23. G. Kulkarni, S. Karan, and A. K. Jha, "Measurement of pure states of light in the orbital-angular-momentum basis using nine multipixel image acquisitions," *Phys. Rev. Appl.* **13**, 054077 (2020).
24. L. Chen, T. Ma, X. Qiu, D. Zhang, W. Zhang, and R. W. Boyd, "Realization of the Einstein-Podolsky-Rosen paradox using radial position and radial momentum variables," *Phys. Rev. Lett.* **123**, 060403 (2019).
25. W. N. Plick and M. Krenn, "Physical meaning of the radial index of Laguerre-Gauss beams," *Phys. Rev. A* **92**, 063841 (2015).
26. A. Trichili, C. Rosales-Guzmán, A. Dudley, B. Ndagano, A. Ben Salem, M. Zghal, and A. Forbes, "Optical communication beyond orbital angular momentum," *Sci. Rep.* **6**, 1–6 (2016).
27. K. Pang, C. Liu, G. Xie, Y. Ren, Z. Zhao, R. Zhang, Y. Cao, J. Zhao, H. Song, H. Song, L. Li, A. N. Willner, M. Tur, R. W. Boyd, and A. E. Willner, "Demonstration of a 10 mbit/s quantum communication link by encoding data on two Laguerre-Gaussian modes with different radial indices," *Opt. Lett.* **43**, 5639–5642 (2018).
28. M. Takeda, W. Wang, Z. Duan, and Y. Miyamoto, "Coherence holography," *Opt. Express* **13**, 9629–9635 (2005).
29. M. Takeda, "Spatial stationarity of statistical optical fields for coherence holography and photon correlation holography," *Opt. Lett.* **38**, 3452–3455 (2013).
30. M. Takeda, W. Wang, D. N. Naik, and R. K. Singh, "Spatial statistical optics and spatial correlation holography: a review," *Opt. Rev.* **21**, 849–861 (2014).
31. S. Aarav, A. Bhattacharjee, H. Wanare, and A. K. Jha, "Efficient generation of propagation-invariant spatially stationary partially coherent fields," *Phys. Rev. A* **96**, 033815 (2017).
32. L. Allen, M. W. Beijersbergen, R. Spreeuw, and J. Woerdman, "Orbital angular momentum of light and the transformation of Laguerre-Gaussian laser modes," *Phys. Rev. A* **45**, 8185 (1992).
33. A. Bhattacharjee, R. Sahu, and A. K. Jha, "Generation of a Gaussian Schell-model field as a mixture of its coherent modes," *J. Opt.* **21**, 105601 (2019).
34. W. Carter and E. Wolf, "Coherence and radiometry with quasihomogeneous planar sources," *J. Opt. Soc. Am.* **67**, 785–796 (1977).
35. A. Starikov and E. Wolf, "Coherent-mode representation of Gaussian Schell-model sources and of their radiation fields," *J. Opt. Soc. Am.* **72**, 923–928 (1982).
36. Q. He, J. Turunen, and A. T. Friberg, "Propagation and imaging experiments with Gaussian Schell-model beams," *Opt. Commun.* **67**, 245–250 (1988).